

## cAMP Increases Apical $I_{sK}$ Channel Current and $K^+$ Secretion in Vestibular Dark Cells

H. Sunose, J. Liu, Z. Shen, D.C. Marcus

Biophysics Laboratory, Boys Town National Research Hospital, 555 North 30<sup>th</sup> St., Omaha, NE 68131, USA

Received: 9 June 1995/Revised: 17 October 1996

**Abstract.** Adenosine 3',5'-cyclic monophosphate (cAMP) is known to stimulate exogenous  $I_{sK}$  channel current in the *Xenopus* oocyte expression system. The present study was performed to determine whether elevation of cytosolic cAMP in a native mammalian epithelium known to secrete  $K^+$  through endogenously expressed  $I_{sK}$  channels would stimulate  $K^+$  secretion through these channels. The equivalent short circuit current ( $I_{sc}$ ) across vestibular dark cell epithelium in gerbil was measured in a micro-Ussing chamber and the apical membrane current ( $I_{sK}$ ) and conductance ( $g_{sK}$ ) of  $I_{sK}$  channels was recorded with both the on-cell macro-patch and nystatin-perforated whole-cell patch-clamp techniques. It has previously been shown that  $I_{sc}$  can be accounted for by transepithelial  $K^+$  secretion and that the apical  $I_{sK}$  channels constitute a significant pathway for  $K^+$  secretion. The identification of the voltage-dependent whole-cell currents in vestibular dark cells was strengthened by the finding that a potent blocker of  $I_{sK}$  channels, chromanol 293B, strongly reduced  $I_{sK}$  from  $646 \pm 200$  to  $154 \pm 22$  pA (71%) and  $g_{sK}$  from  $7.5 \pm 2.6$  to  $2.8 \pm 0.4$  nS (53%). Cytoplasmic cAMP was elevated by applying dibutyryl cyclic AMP (dbcAMP), or the phosphodiesterase inhibitors 3-isobutyl-1-methylxanthine (IBMX) and Ro-20-1724. dbcAMP (1 mM) increased  $I_{sc}$  and  $I_{sK}$  from  $410 \pm 38$  to  $534 \pm 40$   $\mu$ A/cm<sup>2</sup> and from  $4.3 \pm 0.8$  to  $11.4 \pm 2.2$  pA, respectively. IBMX (1 mM) caused transient increases of  $I_{sc}$  from  $415 \pm 30$  to  $469 \pm 38$   $\mu$ A/cm<sup>2</sup> and Ro-20-1724 (0.1 mM) from  $565 \pm 43$  to  $773 \pm 58$   $\mu$ A/cm<sup>2</sup>. IBMX increased  $I_{sK}$  from  $5.5 \pm 1.5$  to  $16.9 \pm 5.8$  pA in on-cell experiments and from  $191 \pm 31$  to  $426 \pm 53$  pA in whole-cell experiments. The leak conductance due to all non- $I_{sK}$  channel sources did not change during dbcAMP and IBMX while 293B in the presence of dbcAMP reduced

$I_{sK}$  by 84% and  $g_{sK}$  by 62%, similar to unstimulated conditions. These results demonstrate that the cAMP pathway is constitutively active in vestibular dark cells and that the cAMP pathway stimulates transepithelial  $K^+$  secretion by increasing  $I_{sK}$  channel current rather than by altering another transport pathway.

**Key words:** Gerbil — On-cell macro-patch clamp — Nystatin-perforated whole-cell patch clamp — Micro-Ussing chamber — Min K channel — Chromanol 293B — Inner ear

### Introduction

The epithelium in the vestibular labyrinth produces a luminal fluid with an unusually high  $[K^+]$  of ca 140 mM [32].  $K^+$  carries the transduction current from the lumen through the sensory hair cells for the detection of acceleration and position. It has been demonstrated that, of the many cell types present in the vestibular epithelium, it is the dark cells which are responsible for secretion of  $K^+$  [29]. The membrane transport proteins responsible for constitutive  $K^+$  secretion by vestibular dark cells have recently been identified. Basolateral uptake of  $K^+$  is mediated by the  $Na^+$ - $K^+$ -ATPase and the  $Na^+$ - $Cl^-$ - $K^+$  cotransporter [29, 59] while  $NaCl$  taken up by the cotransporter recirculates across the basolateral membrane via the  $Na^+$ - $K^+$ -ATPase and  $Cl^-$  channels [31].

Cytosolic  $K^+$  is secreted into the luminal compartment by electrodiffusion through  $I_{sK}$  (or min K) channels in the apical membrane [27]. This channel is characterized by a slow time course of activation by depolarization (order of seconds) and a slow deactivation by hyperpolarization (order of tenths of seconds). The  $I_{sK}$  message has been cloned from various tissues such as kidney, heart and uterus [45]. In the *Xenopus* oocyte expression system, adenosine 3',5'-cyclic monophosphate (cAMP) has been reported to increase  $I_{sK}$  channel

current [6, 51], even though the channel protein itself has no consensus sequence for phosphorylation by cAMP-dependent protein kinase (PKA) [20].

The functional  $I_{sK}$  channel is thought to be composed of two  $I_{sK}$  protein subunits of only 130 amino acids each with a single transmembrane domain and of another unidentified subunit [48, 53]. It is still controversial whether the  $I_{sK}$  protein itself forms the conductive channel or whether  $I_{sK}$  performs a modulatory function [5, 50, 54]. In either case, the  $K^+$  currents in the apical membrane of VDC have a great many properties in common with the currents of other cells expressing either endogenous or exogenous  $I_{sK}$  protein. For simplicity and consistency with the literature, we term the underlying entity the  $I_{sK}$  channel.

In many secretory epithelia, transepithelial ion transport is under hormonal control and this regulation is often mediated by cytoplasmic 2nd messengers, such as cAMP [33]. In the vestibular labyrinth, several observations suggested that cAMP may play a role as a 2nd messenger. In frog semicircular canal, adenylate cyclase activity was demonstrated on the apical and basolateral membrane of dark cells and forskolin, an activator of adenylate cyclase, increased cAMP production [16]. In addition, strial marginal cells (which are cochlear cells closely homologous to vestibular dark cells (*for review*, [55])) have been shown to possess a cAMP 2nd-messenger pathway and a  $Cl^-$  channel regulated by PKA [38, 41].

The aim of the present study was to test the hypothesis that transepithelial electrogenic secretion of  $K^+$  is regulated by cytosolic cAMP and that the regulated  $K^+$  current is carried by the  $I_{sK}$  channels in the apical cell membrane. Transepithelial  $K^+$  secretion was monitored as equivalent short circuit current ( $I_{sc}$ ) [26, 29]. The  $I_{sK}$  channel pathway was observed with both the on-cell macro-patch and nystatin-perforated whole-cell clamp techniques. The cAMP pathway was stimulated by two maneuvers: addition of the membrane-permeable analogue of cAMP, dibutyryl cyclic AMP (dbcAMP), and inhibition of hydrolysis of endogenous cAMP with the phosphodiesterase inhibitors 3-isobutyl-1-methylxanthine (IBMX) and Ro-20-1724.

## Materials and Methods

### TISSUE PREPARATION

Mongolian gerbils (4 to 10 weeks old) were decapitated and temporal bones were removed after anesthesia with intraperitoneal injection of sodium pentobarbital (50 mg/kg). Strips of dark cell epithelium were dissected at 4°C from ampullae of semicircular canals as previously described [60].

### MICRO-USSING CHAMBER

The methods were described previously [26]. Briefly, tissue was placed in a micro-Ussing chamber and the seal to the aperture (80  $\mu$ m

diameter) between two hemi-chambers was made with the apical side of the vestibular dark cell epithelium. The apical and basolateral sides of the tissue were perfused independently and exchange of solution (37°C) on each side was complete within 1 sec. Transepithelial voltage ( $V_t$ ) was measured between calomel electrodes connected to the hemi-chambers via flowing 1 M KCl bridges. Transepithelial resistance ( $R_t$ ) was obtained from the voltage change induced by current pulses (50 nA for 34 msec at 0.3 Hz). Sample and hold circuitry was used to obtain a signal proportional to  $R_t$ . Both  $R_t$  and  $V_t$  were digitally sampled at 1.6 Hz and the corresponding values divided to obtain an apparently continuous plot of the equivalent short circuit current ( $I_{sc}$ ), which was derived from  $V_t$  and  $R_t$  ( $I_{sc} = V_t/R_t$ ).  $I_{sc}$  and  $R_t$  were normalized for the area defined by the aperture of the micro-Ussing chamber. Tissues with either  $V_t$  less than 4 mV or a drift of  $R_t$  more than 1.0  $\Omega$ -cm<sup>2</sup> within 2 min before applying agents were excluded from the data. Experimental agents were applied to the basolateral side for 5 min and subsequently washed out for 4.5 min. The values of  $V_t$ ,  $R_t$  and  $I_{sc}$  just prior to perfusion of dbcAMP, IBMX or Ro-20-1724 were used as control, those at the end of perfusion of the test compound were taken as the experimental value and those at the end of the washout period taken to represent the extent of recovery. Peak transient values for IBMX and Ro-20-1724 were also measured.

### ON-CELL MACRO-PATCH RECORDING

Even though individual  $I_{sK}$  channel openings are not easily resolvable and the single-channel conductance is thought to be small [40, 42], a large patch electrode integrates over enough of the dark cell membrane to yield measurements of a macroscopic  $I_{sK}$  channel current [27, 39, 40, 57]. A strip of epithelium was folded into a loop with the apical membrane facing outward and was continuously perfused (37°C). The working volume of the chamber was 40  $\mu$ l and the flow rate of the perfusate was 2 ml/min, ensuring exchange of solution 0.8 times/sec. The tip of the patch pipette (cAMP & IBMX: 2–3  $\mu$ m; 293B + cAMP: 4–6  $\mu$ m, i.d.) was coated with a 2:1 mixture of  $\alpha$ -tocopherol acetate and heavy mineral oil (Sigma Chemical). The patch-clamp amplifier (Model 3900, Dagan) was connected to the bath with a reference electrode consisting of a Ag/AgCl wire and a flowing 1 M KCl ceramic junction. Seals to the membrane typically had a resistance of 8 gigaohm. The current was low-pass filtered at 1,000 Hz and filtered currents were digitized to 12-bits resolution at a sampling rate of 35.7 kHz for the short voltage steps used to obtain the current-voltage ( $I$ - $V$ ) relationships and 500 Hz for the long hyperpolarization voltage step.

The voltage protocol and method of analysis was the same as previously described [39, 57] and is similar to that described below for the whole-cell recordings. It was designed to obtain measurements of the  $I_{sK}$  current ( $I_{sK}$ ) and conductance ( $g_{sK}$ ) at 0 mV holding potential ( $V_{hold}$ ), the reversal voltage of the membrane patch ( $V_r$ ) and the time constant of deactivation ( $\tau_{off}$ ).  $I_{sK}$  and  $g_{sK}$  were corrected for leak current  $I_{leak}$  and leak conductance ( $g_{leak}$ ). The reversal voltage of the apical membrane is  $V_r$  plus the cell membrane voltage with respect to the bath, which is ca -18 mV [60]. These parameters were obtained in 15-sec intervals (Figs. 6, 7 and 11) throughout each experiment. Briefly, the pipette was held at 0 mV with respect to the bath and a tail-current  $I$ - $V$  plot was created from four brief test pulses. The membrane conductance and reversal voltage were obtained from the  $I$ - $V$  plot. Hyperpolarizing to -40 mV has been shown to deactivate the dark cell  $I_{sK}$  channel [27]. Following a hyperpolarization to -40 mV for 2 or 4 sec, the pipette was returned to 0 mV.

The currents at the end of the hyperpolarizing step and the current immediately after return to 0 mV (while the  $I_{sK}$  channels were still deactivated) were used to estimate the leak conductance and leak current at 0 mV. The net current and conductance of the  $I_{sK}$  channels,  $I_{sK}$

and  $g_{sK}$  were obtained by correcting for these leak estimates. The reversal voltage,  $V_r$ , represented the composite influence of the  $I_{sK}$  channels along with all other leak pathways present including the patch seal. This was taken as an indicator of the relative contribution of the  $I_{sK}$  channels to the patch conductance.

The time constant of deactivation,  $\tau_{off}$ , was obtained by fitting the current measurements during the long hyperpolarizing voltage step with a single exponential (current =  $A \cdot \exp(-t/\tau_{off}) + C$ , where  $A$  is the amplitude,  $t$  the time and  $C$  the asymptote). Data were fitted by the method of Chebyshev (Clampfit, version 6.01, Axon Instruments Foster City, CA). Values for  $\tau_{off}$  were accepted and included in the average according to previously established criteria [57].

IBMX and dbcAMP were applied for 5 min and washed out for 5 min. Data were excluded when (1) the cells showed during the control period either no measurable deactivation current during the long hyperpolarizing step or (2) the membrane conductance drifted more than 30 pS within 2 min before applying testing agents. Values for  $I_{sK}$ ,  $g_{sK}$ ,  $V_r$  and  $\tau_{off}$  were obtained for the control, response to dbcAMP or IBMX and washout by averaging the four values during the 1 min immediately prior to drug application, at the end of drug application and 4 min after cessation of drug application, respectively. In some cases, the initial control period was extended by 1 min in order to obtain sufficient points meeting the acceptance criteria for the estimation of  $\tau_{off}$ . The patch pipette was perfused as previously described [39].

#### NYSTATIN-PERFORATED WHOLE-CELL PATCH RECORDING

The nystatin-perforated whole-cell patch clamp technique was chosen over the conventional whole-cell technique to avoid run-down of  $I_{sK}$  channel activity due to loss of regulatory compounds from the cytosol [27]. Experiments were conducted in the absence of  $Cl^-$  to increase the ratio between the cell membrane resistance and the access resistance, a necessary condition to effectively clamp the membrane potential in these cells. An unusually high  $Cl^-$  conductance in the basolateral membrane of these cells is responsible for an unusually low membrane resistance of typically 20 Megohm per cell in the presence of  $Cl^-$  [31, 60].

Recording was similar to the on-cell macropatch experiments except that the tip of the patch pipette was uncoated and the internal diameter was 1 to 2  $\mu m$  with a resistance of 8-to-12 Megohm in the  $Cl^-$ -free bath solution. The tip was filled with a  $Cl^-$ -free solution containing 200  $\mu g/ml$  nystatin. The rest of the pipette was backfilled with a solution containing 15 mM  $Cl^-$  to stabilize the potential of the Ag/AgCl wire. Typically, the perforated whole-cell configuration was established within 10 min after obtaining a giga-ohm seal. The access resistance after perforation averaged  $32 \pm 2$  Mohm ( $n = 11$ ) which was compensated by  $60 \pm 7\%$ . The cell membrane resistance was  $>100$  Megohm in the absence of  $Cl^-$  with about half of the conductance attributed to the  $I_{sK}$  channels at  $V_{hold} = 0$  mV.

The experimental protocol was similar to that used for on-cell recordings and is illustrated in Fig. 1. The cell voltage was held at 0 mV and the  $I_{sK}$  channels were deactivated every 30 sec by a long (2-to-4-sec) hyperpolarizing voltage at  $-50$  mV which was preceded and followed by brief voltage steps (cell with respect to the bath) of 45, 0,  $-45$  and  $-90$  mV (20 msec each) to obtain tail-current  $I$ - $V$  relationships with and without activity of the  $I_{sK}$  channels. The numbers adjacent to the current trace in Fig. 1B identify the values used in obtaining these parameters. Tail currents were measured after capacitive transients had subsided.

The current through the  $I_{sK}$  channels at  $V_{hold} = 0$  mV ( $I_{sK}$ ) was the difference between the amplitude of the outward currents at  $V_{hold} = 0$  mV and that following the long hyperpolarization (Fig. 1B: (1) minus (12)). The conductance of  $I_{sK}$  channels at  $V_{hold} = 0$  mV ( $g_{sK}$ ) was the

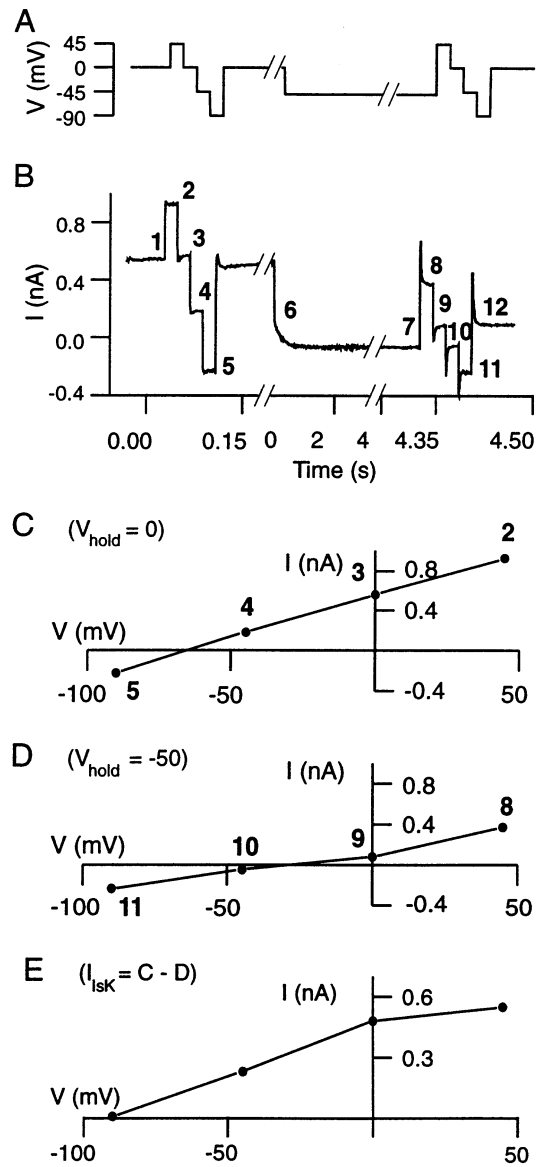


**Fig. 1.** Voltage protocol and analysis of  $I_{sK}$  channel current, conductance and reversal voltage for nystatin-perforated whole-cell patch clamp recordings. (A) Voltage protocol; time scale same as in B. (B) The  $I_{sK}$  current ( $I_{sK}$ ) at a holding voltage ( $V_{hold}$ ) of 0 mV is derived from the current at point 1 corrected for the leak current at point 12. The  $I_{sK}$  channel conductance at 0 mV ( $g_{sK}$ ) is derived from the slope of the tail-current  $I$ - $V$  relationship (points 3, 4 and 5) corrected for the leak conductance (from points 9, 10 and 11). The reversal voltage ( $V_r$ ) was interpolated from the tail-current  $I$ - $V$  relationship.  $\tau_{off}$  was obtained from fitting an exponential relation to the current between points 6 and 7. (C) Tail-current  $I$ - $V$  relationship,  $V_{hold} = 0$ ; (D) Tail-current  $I$ - $V$  relationship,  $V_{hold} = -50$ ; (E)  $I_{sK}$  channel  $I$ - $V$  relationship,  $(C-D)$ .

difference of the membrane conductances at 0 mV and  $V_{hold} = -50$  mV calculated by the linear regression of the  $I$ - $V$  relationships between 0 mV and  $-90$  mV (difference between slopes of points 3 to 5 in Fig. 1C and 9 to 11 in Fig. 1D). The reversal voltage at  $V_{hold} = 0$  mV ( $V_r$ ) was calculated by the linear regression of the  $I$ - $V$  relationship between

0 mV and  $-90$  mV (Fig. 1C). The  $I$ - $V$  relationship of the leak-corrected  $I_{SK}$  current (Fig. 1E) was obtained from the difference of the two  $I$ - $V$  relationships at  $V_{hold} = 0$  and  $-50$  mV (Fig. 1C minus Fig. 1D). The reversal voltage of the  $I_{SK}$  current ( $V_{r,Isk}$ ) was obtained from the averaged  $I$ - $V$  relationships of the leak-corrected  $I_{SK}$  current (Fig. 1E).

The current recorded during the long hyperpolarizing voltage sometimes had an upward slope following deactivation of the  $I_{SK}$  current. Therefore, the time constant of deactivation ( $\tau_{off}$ ) was obtained by fitting the current measurements during the initial 1 sec of the hyperpolarizing voltage step with a single exponential function containing an additive linear term to account for the sloping baseline:

$$\text{Current} = A \cdot \exp(-t/\tau_{off}) + Dt + C,$$

where  $A$  is the amplitude,  $t$  the time,  $D$  the slope and  $C$  the asymptote. Data were fitted by the method of Chebyshev (Clampfit, version 6.01, Axon Instruments). The linear component was thought to be the result of a small remaining pool of cytosolic  $Cl^-$  (or  $HCO_3^-$ ) which was being pushed out by the hyperpolarizing voltage. When this component occurred, it diminished during the course of the experiment, consistent with the view that  $Cl^-$  was being lost from the cell. This imperfection in the space-clamping of  $Cl^-$  is to be expected from the lower permeability of nystatin to  $Cl^-$  than to cations.

To stimulate the cAMP pathway, dbcAMP was applied for 5 min and washed out for 5 min. Cells were excluded which showed during control conditions no deactivating outward current at the beginning of the 4-sec hyperpolarization. The reported measurements are averages of  $I_{Isk}$ ,  $g_{Isk}$ ,  $V_r$  and  $\tau_{off}$  from 1 to 0.5 min before drug application, from 4.5 to 5 min after the onset of drug application and from 4.5 to 5 min after washout and taken as the values for the control, the response and the washout, respectively. The  $I$ - $V$  relationships from the same time periods were averaged and presented in Fig. 10. In the whole-cell experiments with 293B, the control values are averages of the 4 data points preceding the drug and the experimental values are the last data point in the presence of 293B.

## SOLUTIONS AND CHEMICALS

In all experiments, both sides of the epithelium were initially bathed in a control solution containing (in mM) 150 NaCl, 1.6  $K_2HPO_4$ , 0.4  $KH_2PO_4$ , 1  $MgCl_2$ , 0.7  $CaCl_2$ , 5 glucose, pH 7.4 at 37°C. The patch pipette solution for on-cell experiments contained 150 NaCl, 3.6 KCl, 1  $MgCl_2$ , 0.7  $CaCl_2$  and 10 4-(2-hydroxyethyl)-piperazine-1-ethanesulfonic acid (HEPES; pH 7.4 at 37°C). In whole-cell experiments, the  $Cl^-$ -free bath solution contained 150 Na-gluconate, 1.6  $K_2HPO_4$ , 0.4  $KH_2PO_4$ , 1  $MgSO_4$ , 4  $Ca$ -(gluconate) $_2$ , 5 glucose, pH 7.4 and  $Cl^-$ -free pipette tip solution contained 150 K-gluconate, 1  $MgSO_4$ , 1 EGTA, 10 Heps, pH 7.2.

IBMX, dbcAMP and dibutylryl cGMP (dbcGMP) were dissolved directly in the control solution while 293B and Ro-20-1724 were pre-dissolved in DMSO just before use; pH was readjusted to 7.4 at 37°C. The final DMSO concentration was 0.1%. IBMX and dbcAMP were purchased from Sigma (St. Louis, MO) and Ro-20-1724 from Calbiochem (La Jolla). The chromanol 293B was a gift from Dr. H.-J. Lang (Hoechst AG, Pharmaceutical Research/G838, Frankfurt am Main, Germany). 293B was dissolved in DMSO and the stock solution stored frozen until use. All other chemicals were purchased from Sigma or Fluka (Ronkonkoma, NY).

## STATISTICS

Data are presented as means  $\pm$  SEM and  $n$  indicates the number of observations. The paired Student's  $t$ -test was employed for statistical analysis and differences were considered to be significant for  $P < 0.05$ .

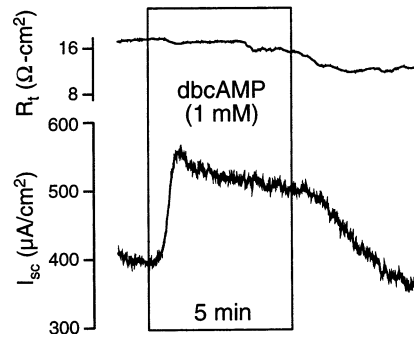


**Fig. 2.** Effect of basolateral perfusion for 5 min of dbcAMP (1 mM) on transepithelial equivalent short circuit current ( $I_{sc}$ ) across vestibular dark cell epithelium. Representative recording.

## Results

### TRANSEPITHELIAL CURRENTS

Under control conditions,  $V_t$ ,  $R_t$  and  $I_{sc}$  (derived from  $V_t$  and  $R_t$ ) were  $6.2 \pm 0.4$  mV,  $12.1 \pm 0.7$   $\Omega$ - $cm^2$  and  $534 \pm 22$   $\mu A/cm^2$ , respectively ( $n = 38$ ), similar to values found in previous studies [26].

The effect of the dbcAMP on transepithelial ion transport by vestibular dark cell epithelium was measured. Basolateral perfusion of 1 mM dbcAMP increased  $V_t$  and  $I_{sc}$  and decreased  $R_t$  with delays of  $27 \pm 4$  sec to the onset of the response and of  $89 \pm 4$  sec until the peak ( $n = 6$ ; Fig. 2).  $V_t$  increased from  $5.9 \pm 0.4$  to  $7.4 \pm 0.6$  mV,  $I_{sc}$  from  $410 \pm 38$  to  $534 \pm 40$   $\mu A/cm^2$  while  $R_t$  decreased by  $0.6 \pm 0.2$   $\Omega$ - $cm^2$  from  $14.8 \pm 1.2$  to  $14.1 \pm 1.0$   $\Omega$ - $cm^2$  ( $n = 6$ ). After the peak,  $V_t$  decreased significantly to  $6.5 \pm 0.5$  mV at 4 to 5 min; this value was still significantly higher than the control.  $I_{sc}$  stayed at  $526 \pm 46$   $\mu A/cm^2$ , which was significantly higher than control; the peak increase in  $I_{sc}$  was  $31.8 \pm 4.5\%$  and at the end of perfusion  $30.0 \pm 7.3\%$  above the control value. Washout for 4.5 min led to a decrease of  $V_t$ ,  $R_t$  and  $I_{sc}$  to  $4.1 \pm 0.2$  mV,  $10.8 \pm 1.0$   $\Omega$ - $cm^2$  and  $400 \pm 52$   $\mu A/cm^2$ , respectively.

To stimulate the cAMP pathway by another means and to test for the constitutive activity of adenylate cyclase in vestibular dark cells, the phosphodiesterase inhibitor IBMX was perfused and found to induce a relatively complicated response (Fig. 3). Under control conditions,  $V_t$ ,  $R_t$  and  $I_{sc}$  in this series were  $6.1 \pm 0.8$  mV,  $13.8 \pm 2.1$   $\Omega$ - $cm^2$  and  $453 \pm 30$   $\mu A/cm^2$ , respectively ( $n = 9$ ). Basolateral perfusion of IBMX (1 mM) initially induced a transient decrease in both  $V_t$  and  $I_{sc}$  with a delay of  $10 \pm 1$  sec, and the low points of  $5.5 \pm 0.6$  mV and  $415 \pm 30$   $\mu A/cm^2$  were reached at  $23 \pm 3$  sec. A significant but transient increase in  $V_t$  and  $I_{sc}$  followed, which had a peak of  $6.2 \pm 0.7$  mV and  $469 \pm 38$   $\mu A/cm^2$ ,

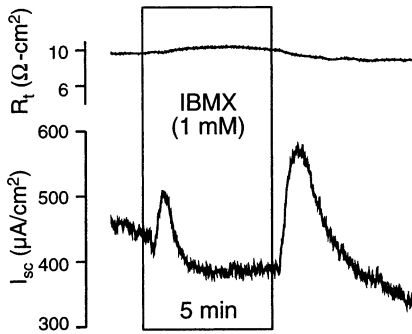


**Fig. 3.** Effect of basolateral perfusion for 5 min of IBMX (1 mM) on  $I_{sc}$  across vestibular dark cell epithelium. Representative recording.

respectively, at  $47 \pm 3$  sec. The positive peak in  $I_{sc}$  was  $12.7 \pm 2.5\%$  above the preceding low points.

$I_{sc}$  subsequently decreased significantly from the peak with  $V_t$  and  $I_{sc}$  declining to  $5.2 \pm 0.4$  mV and  $411 \pm 29$   $\mu\text{A/cm}^2$ , respectively, at the end of IBMX. No significant change in  $R_t$  was observed in the presence of IBMX ( $14.1 \pm 2.2$   $\Omega\text{-cm}^2$  at the initial valley,  $14.0 \pm 2.1$   $\Omega\text{-cm}^2$  at the peak and  $13.1 \pm 1.4$   $\Omega\text{-cm}^2$  at the end).  $I_{sc}$  at the end of perfusion of IBMX was  $8.9 \pm 3.5\%$  below the control value. Washout of IBMX caused transient but significant increases in  $V_t$  and  $I_{sc}$  to  $7.3 \pm 0.6$  mV and  $646 \pm 34$   $\mu\text{A/cm}^2$ , respectively, which were accompanied by a transient significant decrease in  $R_t$  to  $11.7 \pm 1.2$   $\Omega\text{-cm}^2$  after  $53 \pm 3$  sec of washout. In the end of the washout,  $V_t$  and  $I_{sc}$  decreased significantly to  $4.4 \pm 0.3$  mV and  $404 \pm 22$   $\mu\text{A/cm}^2$ , respectively although  $R_t$  did not change significantly ( $11.4 \pm 1.2$   $\Omega\text{-cm}^2$ ).

IBMX is known to inhibit several subtypes of phosphodiesterase [4, 62]. Although the increase in  $I_{sc}$  is consistent with an increase in cAMP, the negative part of the response to IBMX could therefore have been due to inhibition of a cGMP-dependent phosphodiesterase and a consequent increase in cytosolic cGMP. We tested this hypothesis in two ways. First, we specifically inhibited cAMP-dependent phosphodiesterase with the agent Ro-20-1724 [21]. Similar to IBMX, basolateral perfusion of Ro-20-1724 (0.1 mM) for 2-to-5 min caused a transient increase in  $V_t$  and  $I_{sc}$  with a concomitant decrease in  $R_t$  (Fig. 4) and similar to dbcAMP the increase occurred with a delay of  $17 \pm 1$  sec and reached its peak at  $45 \pm 2$  sec ( $N = 7$ ).  $V_t$  increased from  $6.3 \pm 0.5$  mV to  $8.0 \pm 0.6$  mV and  $I_{sc}$  increased by  $37 \pm 2\%$  from  $565 \pm 43$  to  $773 \pm 58$   $\mu\text{A/cm}^2$  ( $n = 7$ ) at the peak.  $R_t$  declined slightly from  $11.2 \pm 0.5$  to  $10.5 \pm 0.4$   $\Omega\text{-cm}^2$  at peak  $I_{sc}$ .

Second, we directly stimulated the cGMP pathway by basolateral perfusion of the membrane-permeant analogue dbcGMP (Fig. 5). There was a minor (3%), but statistically significant, transient increase by  $17 \pm 5$   $\mu\text{A/cm}^2$  in  $I_{sc}$  from  $618 \pm 29$  to  $635 \pm 28$   $\mu\text{A/cm}^2$  at  $20 \pm 2$  sec ( $n = 15$ ). At the end of the perfusion,  $I_{sc}$  had declined to  $592 \pm 29$   $\mu\text{A/cm}^2$  which is only 4% less than

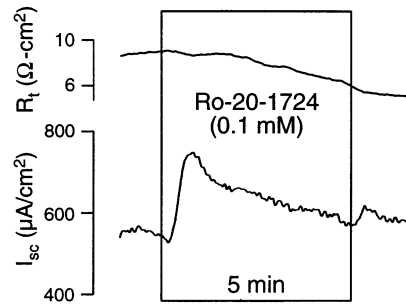


**Fig. 4.** Effect of basolateral perfusion for 5 min of Ro-20-1724 (0.1 mM) on  $I_{sc}$  across vestibular dark cell epithelium. Representative recording.

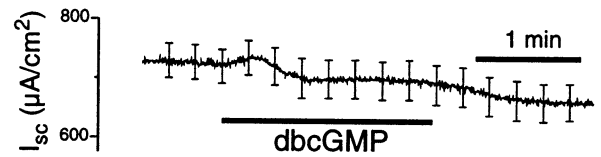


**Fig. 5.** Summary of measurements of  $I_{sc}$  showing the effect of basolateral perfusion for 2 min of dbcGMP (1 mM) on  $I_{sc}$  across vestibular dark cell epithelium. Mean  $\pm$  SEM ( $n = 15$ ).

the control level but statistically significant. These changes in  $I_{sc}$  were small compared to either the initial increase or subsequent decrease of  $I_{sc}$  during IBMX. These data argue that the cGMP pathway exerts little control over  $I_{sc}$  and that the biphasic response to inhibition of phosphodiesterase is more likely a feedback effect within the cAMP pathway or interaction with another signal pathway.

#### ON-CELL MACROPATCH CURRENTS

Under control conditions,  $I_{sK}$ ,  $g_{sK}$ ,  $V_r$  and  $\tau_{off}$  were  $4.9 \pm 0.8$  pA,  $85 \pm 13$  pS,  $-39.8 \pm 2.8$  mV ( $n = 16$ ) and  $452 \pm 35$  msec ( $n = 8$ ). The values of  $V_r$  and  $\tau_{off}$  are similar to those found in a previous study [57] but the values of  $I_{sK}$  and  $g_{sK}$  are substantially lower due to the smaller area of membrane sampled in the present study.

Bath perfusion of dbcAMP (1 mM) significantly increased  $I_{sK}$ ,  $g_{sK}$  and  $V_r$  from  $4.3 \pm 0.8$  to  $11.4 \pm 2.2$  pA, from  $75 \pm 16$  to  $169 \pm 25$  pS and from  $-35.8 \pm 4.1$  to  $-48.2 \pm 4.0$  mV (Fig. 6;  $n = 8$ ). The shift of  $V_r$  toward a more negative value (closer to the equilibrium potential for  $K^+$ ) and the increases in  $I_{sK}$  and  $g_{sK}$  are consistent with an increasing contribution of the  $I_{sK}$  channel conductance to that of the apical membrane.  $g_{leak}$  and  $\tau_{off}$  remained unchanged during dbcAMP (control vs. response;  $80 \pm 12$  pS vs.  $86 \pm 14$  pS,  $n = 8$ ;  $404 \pm 50$  msec vs.  $384 \pm 48$  msec,  $n = 4$ ). The effects on  $I_{sK}$ ,  $g_{sK}$  and  $V_r$  were not reversible during the first 5 min of washout

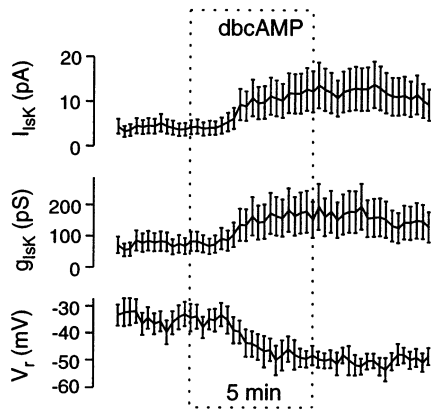


**Fig. 6.** Summary of on-cell macro-patch clamp recordings of apical membrane parameters ( $I_{sK}$ ,  $g_{sK}$ , and  $V_r$ ) of vestibular dark cells during 5 min bath perfusion of dbcAMP (1 mM). Mean  $\pm$  SEM ( $n = 8$ ).

( $10.9 \pm 2.1$  pA,  $145 \pm 20$  pS and  $-49.7 \pm 3.1$  mV, respectively;  $n = 8$ ).

Bath perfusion of IBMX (1 mM) increased  $I_{sK}$ ,  $g_{sK}$  and  $V_r$  significantly from  $5.5 \pm 1.5$  to  $16.9 \pm 5.8$  pA, from  $96 \pm 22$  to  $223 \pm 62$  pS and from  $-43.8 \pm 3.5$  to  $-55.6 \pm 6.4$  mV, respectively (Fig. 7;  $n = 8$ ).  $g_{leak}$  and  $\tau_{off}$  remained unchanged (control vs. response;  $64 \pm 6$  pS vs.  $77 \pm 9$  pS,  $n = 8$ ;  $501 \pm 39$  msec vs.  $484 \pm 77$  msec,  $n = 4$ ). No significant changes occurred during washout ( $15.0 \pm 6.8$  pA,  $201 \pm 72$  pS and  $-53.7 \pm 4.7$  mV, respectively;  $n = 8$ ).

#### NYSTATIN-PERFORATED WHOLE-CELL CURRENTS

The nystatin-perforated whole-cell patch clamp technique under  $Cl^-$ -free conditions permitted the observation of  $I_{sK}$  channel activity for more than 15 min in vestibular dark cells. The cell membrane carried an outward current at  $V_{hold} = 0$  mV which had a slowly deactivating component at the beginning of the long hyperpolarization, attributed to  $I_{sK}$  channel activity (Fig. 1B). The outward current at  $V_{hold} = 0$  mV was inhibited by the long hyperpolarization. The  $I$ - $V$  relationship (Fig. 1C) had a negative reversal voltage in accordance with the  $K^+$  selectivity of the membrane. Decreases of the membrane conductance and the reversal voltage were observed at  $V_{hold} = -50$  mV (Fig. 1D). The resulting  $I$ - $V$  relationship of the leak-subtracted current (Fig. 1E) showed a highly negative reversal voltage, consistent with a high  $K^+$  selectivity of the  $I_{sK}$  channel.

The chromanol 293B is a potent blocker of  $I_{sK}$  channel exogenously expressed in *Xenopus* oocytes and endogenous  $I_{sK}$  channels in strial marginal cells [40, 44]. Whole-cell recordings were made in vestibular dark cells and 293B ( $10^{-5}$  M) added to the bath perfusate (Fig. 8).  $I_{sK}$  and  $g_{sK}$  decreased by 71% from  $646 \pm 200$  to  $154 \pm 22$  pA and by 53% from  $7.5 \pm 2.6$  to  $2.8 \pm 0.4$  nS,

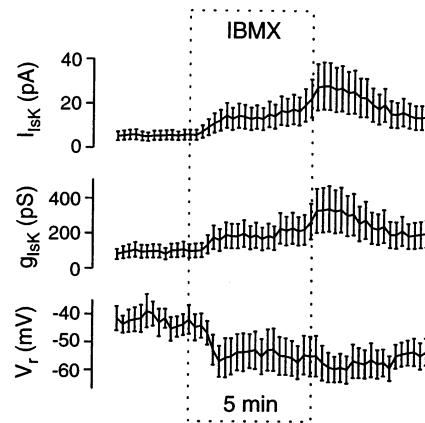


**Fig. 7.** Summary of on-cell macropatch clamp recordings of  $I_{sK}$ ,  $g_{sK}$ , and  $V_r$  of vestibular dark cells during 5 min bath perfusion of IBMX (1 mM). Mean  $\pm$  SEM ( $n = 8$ ).

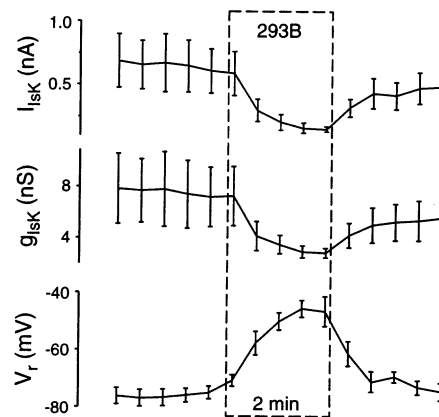


**Fig. 8.** Summary of whole-cell patch clamp recordings of  $I_{sK}$ ,  $g_{sK}$ , and  $V_r$  of vestibular dark cells during 2 min bath perfusion of 293B ( $10^{-5}$  M). Mean  $\pm$  SEM ( $n = 7$ ).

respectively.  $V_r$  decreased from  $-76.1 \pm 2.52$  to  $-46.6 \pm 5.14$  ( $N = 4$ ) and the effects were partially reversible.  $I_{leak}$  and  $g_{leak}$  remained unchanged (control vs. response;  $134 \pm 20$  vs.  $139 \pm 21$  pA and  $3.4 \pm 0.2$  vs.  $3.6 \pm 0.2$  nS,  $N = 4$ ).

The cell capacitance was  $47 \pm 4$  pF ( $n = 11$ ). The large capacitances observed in the present study are consistent with the large membrane area due to extensive basolateral infoldings which are preserved in our preparation. The capacitance would be expected to be about 33–49 pF under the assumptions that the apical membrane is 2 to 3% of total plasma membrane, the diameter of the apical membrane is 11  $\mu$ m and the specific membrane capacitance is  $1 \mu$ F/cm<sup>2</sup> [15]. In contrast, the capacitance of a simple sphere having a diameter of 10  $\mu$ m would be only 3 pF. The lower single-cell capacitance observed in isolated cells may be due to partial loss of basolateral infoldings during isolation [46].

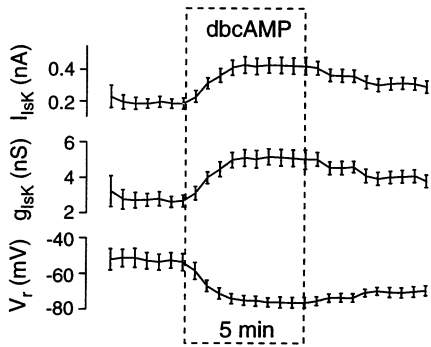


**Fig. 9.** Summary of whole-cell patch clamp recordings of  $I_{IsK}$ ,  $g_{IsK}$  and  $V_r$  of vestibular dark cells during 5 min bath perfusion of dbcAMP (1 mM). Mean  $\pm$  SEM ( $n = 7$ ).

Application of dbcAMP (1 mM) to vestibular dark cells increased  $I_{IsK}$ ,  $g_{IsK}$  and  $V_r$  from  $191 \pm 31$  to  $426 \pm 53$  pA,  $2.71 \pm 0.35$  to  $5.07 \pm 0.50$  nS, and  $-53.2 \pm 4.4$  to  $-76.2 \pm 2.9$  mV (Fig. 9;  $n = 7$ ).  $\tau_{off}$  remained unchanged ( $196 \pm 13$  vs.  $195 \pm 19$  msec;  $n = 7$ ). Subsequent washing for 5 min caused a significant decrease of  $I_{IsK}$ ,  $g_{IsK}$  and  $V_r$  from the end of stimulation ( $I_{IsK}$ ,  $308 \pm 38$  pA;  $g_{IsK}$ ,  $3.99 \pm 0.34$  nS;  $V_r$ ,  $-69.5 \pm 2.8$  mV;  $n = 7$ ). Application of dbcAMP to vestibular dark cells changed the  $I$ - $V$  relationship at  $V_{hold} = 0$  mV (Fig. 10A), while affecting little the  $I$ - $V$  relationship at  $V_{hold} = -50$  mV (Fig. 10B). The  $I$ - $V$  relationship of the  $I_{sK}$  channel (Fig. 10C) displayed after dbcAMP an increased conductance at all voltages while the reversal voltage,  $V_{r,IsK}$ , remained highly negative, increasing from  $-76.3 \pm 3.4$  in control vs.  $-92.4 \pm 2.0$  mV after dbcAMP ( $n = 7$ ). The predicted Nernstian reversal voltage for a purely  $K^+$ -selective membrane was  $-98$  mV. The control value of  $-76$  probably reflects imperfect deactivation of the  $I_{sK}$  channels by hyperpolarization and a minor contribution of the  $Cl^-$  conductance. It is not possible to perfectly eliminate the anion conductance since most epithelial  $Cl^-$  channels have been found to be partially permeable to  $HCO_3^-$  [22], a ubiquitous product of aerobic metabolism.

#### INHIBITION OF BOTH CONSTITUTIVE AND CAMP-STIMULATED $I_{sK}$ CHANNEL CURRENTS BY 293B

Similar effects on  $I_{IsK}$ ,  $g_{IsK}$  and  $V_r$  were seen as in the previous series of on-cell macro patch measurements in response to addition of dbcAMP (1 mM) to the bath. In the present series (Fig. 11), dbcAMP caused  $I_{IsK}$  to increase from  $5.1 \pm 1.1$  to  $24.5 \pm 6.2$  pA,  $g_{IsK}$  from  $243 \pm 60$  to  $537 \pm 112$  pS and  $V_r$  from  $-24.7 \pm 5.0$  to  $-38.6 \pm 4.4$  mV ( $n = 5$ ).

Perfusion of 293B through the patch pipette on the apical membrane (Fig. 11) caused a decrease of  $I_{IsK}$  by  $84.1 \pm 2.9\%$  (to  $4.2 \pm 1.7$  pA),  $g_{IsK}$  by  $61.8 \pm 11.5\%$  (to  $192 \pm 51$  pS) and  $V_r$  to  $-22.4 \pm 3.6$  mV ( $n = 5$ ). The

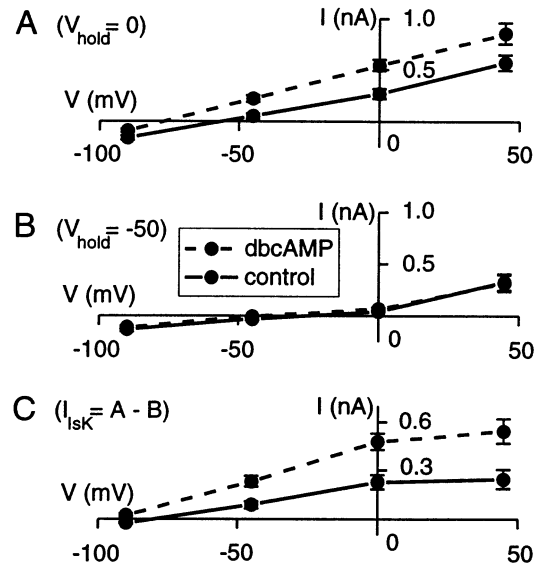


**Fig. 10.** Summary of  $I$ - $V$  relationships for whole-cell patch clamp recordings of  $I_{IsK}$ ,  $g_{IsK}$  and  $V_r$  of vestibular dark cells in the presence (broken line) and absence (continuous line) of dbcAMP (1 mM). Mean  $\pm$  SEM ( $n = 7$ ).

fractional decreases of the composite  $I_{IsK}$  and  $g_{IsK}$  are similar to those reported above under unstimulated conditions.

## Discussion

### $I_{sc}$ AND $I_{sK}$ CHANNEL CURRENTS

The relationship between electrogenic  $K^+$  secretion, represented by the transepithelial equivalent short-circuit current,  $I_{sc}$ , and the slowly-activating, voltage-dependent currents measured with the on-cell macro-patch clamp technique has been demonstrated previously [27, 29]. The identification of the patch clamp currents as originating from  $I_{sK}$  channels is based on several observations and comparisons to endogenous  $I_{sK}$  channels in cardiac myocytes and exogenous  $I_{sK}$  channels in *Xenopus* oocytes.

The most obvious similarities are the time constants of activation and deactivation with membrane voltage and the  $K^+$  selectivity [10, 19, 27, 51]. Estimates of single-channel conductance by fluctuation analysis are also comparable; 1.6 pS for vestibular dark cells [40] and 1.3 to 6 pS for cardiac myocytes [17, 49]. Curiously, exogenous  $I_{sK}$  channels expressed in *Xenopus* oocytes produce fluctuations with amplitudes several orders of magnitude less than those seen in dark cells or myocytes [63].

Regulation of the vestibular dark cell current is also strikingly similar to  $I_{sK}$  channels in other systems: up-

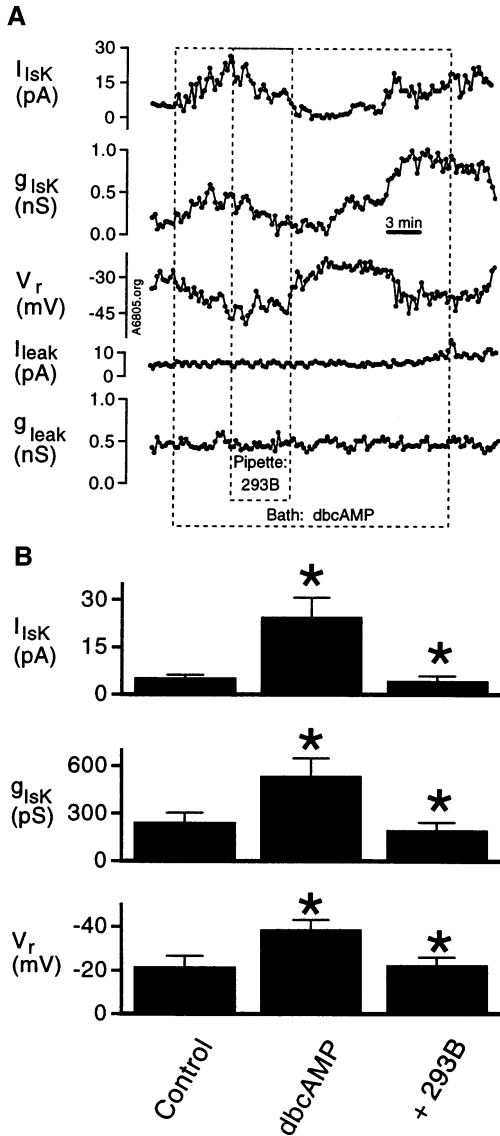


**Fig. 11.** Effect of patch perfusion of 293B (10  $\mu$ M) on cAMP-stimulated (1 mM dbcAMP) apical membrane currents in vestibular dark cells. (A) Example of reversible inhibition by 293B on  $I_{sK}$ ,  $g_{sK}$  and  $V_r$ ; there was no effect on  $I_{leak}$  and  $g_{leak}$ . (B) Summary; mean  $\pm$  SEM ( $n = 5$ ).

regulation by cAMP (vide infra) [6], cytosolic  $Ca^{2+}$  [10, 25] and hypotonic challenge [11, 57] and downregulation by protein kinase C [25, 30, 51, 64]. The currents are not due to maxi- $K^+$  channels found in the apical membrane at low density since patch excision results in rundown of the slowly-activating, voltage-dependent currents whereas the maxi- $K^+$  channels were stimulated by the same maneuver [27, 47]. Pharmacologic intervention is also similar. Currents in vestibular dark cells are stimulated by the disulfonic stilbene 4,4'-diisothiocyanatostilbene-2,2'-disulfonic acid (DIDS) [9, 39] (although, see Attali et al., [2]) and inhibited by the new, potent  $I_{sK}$

channel blocker 293B (Fig. 8) [40, 44]. Recently,  $I_{sK}$  "knockout" mice were raised which displayed severe vestibular disorders and had dramatically collapsed endolymphatic spaces in all regions of the inner ear including the vestibular labyrinth. The  $I_{sc}$  was virtually absent across the vestibular dark cell epithelium in these animals [52].

Finally, several observations on the homologous cells in the cochlea, strial marginal cells, are consistent with an identification of  $I_{sK}$  channels in these epithelia. The  $I_{sK}$  channel protein has been immunolocalized to the apical membrane of guinea pig and rat strial marginal cells [34, 37]. Further, recent results of RT-PCR and sequence analysis of gerbil stria vascularis has shown mRNA sequences of the expected length and composition for  $I_{sK}$  channel message using primers designed from the known sequences of other rodents (rat and mouse) [28]. Taken together, there is little doubt that the slowly-activating, voltage-dependent currents reported here originated from  $I_{sK}$  channels in the apical membrane.

#### STIMULATION OF $I_{sc}$ AND $I_{sK}$ CHANNEL CURRENTS BY CAMP

The increase in  $I_{sc}$  during activation of the cAMP pathway with dbcAMP could be due to one or more of several factors. The primary effect of elevated cytosolic cAMP is apparently on a cellular ion transport process rather than the paracellular pathway since both dbcAMP and IBMX increased the  $I_{sK}$  channel current,  $I_{sK}$ . It has been proposed that elevation of cytoplasmic cAMP regulates the resistance of the paracellular pathway in other epithelia [3, 14]. If cAMP regulates the paracellular pathway in dark cell epithelium, it is a relatively slow and small effect.

The question arises whether the cAMP pathway acts directly on a transport pathway involved in constitutive  $K^+$  secretion or whether there are other intermediaries. The fact that there was a substantial delay after the onset of perfusion of dbcAMP, IBMX and Ro-20-1724 speaks in favor of a cytosolic effect via a relatively lengthy signal pathway. The increase in  $I_{sc}$  apparently was solely via an increase in the current through the  $I_{sK}$  channel since the  $I_{sK}$  channel inhibitor 293B reduced  $I_{sK}$  and  $g_{sK}$  similarly during cAMP-stimulated and unstimulated conditions and since there was no significant change in the apical membrane leak conductance during either dbcAMP or IBMX. The increases in  $I_{sK}$ ,  $g_{sK}$  and  $V_r$  during dbcAMP and IBMX are consistent with one or more underlying cellular mechanisms: an effect of cAMP (or PKA) (1) directly on the  $I_{sK}$  channel protein, (2) on another transporter which indirectly increases  $I_{sK}$  through changes in membrane potential or cytosolic ion concentration or (3) on a membrane traffic pathway



to control the number of  $I_{sK}$  channels in the apical plasma membrane.

Activation by the cAMP pathway could be a direct effect on the  $I_{sK}$  channel since cAMP has been described as an activator of  $I_{sK}$  channels in the *Xenopus* oocyte expression system [6, 51]. Even though the channel protein itself has no consensus sequence for phosphorylation by PKA [20], lack of the consensus sequence for PKA does not exclude the possibility of direct activation by this kinase. An increase of CFTR channel activity by PKA after mutagenesis of all known PKA phosphorylation site consensus sequences suggested that other phosphorylation sites for PKA exist on some membrane proteins [12]. Therefore, direct activation remains a candidate to explain the observed effects.

Indirect activation of  $I_{sK}$  by membrane voltage,  $[K^+]_i$  or  $pH_i$  is not likely. Activation of either the basolateral  $Na^+-K^+-ATPase$  or  $Na^+-Cl^- -K^+$  cotransporter by cAMP would be expected to increase cytoplasmic  $[K^+]$ . It has indeed been found that cAMP via PKA modulates the activity of both of these transporters in other cells, although the direction of the regulation varies with the cell types and species studied [8, 18]. However, dbcAMP stimulated  $I_{sK}$  in the whole-cell experiments as well as in on-cell macro-patch clamp recordings. Under whole-cell conditions the membrane voltage and cytosolic  $[K^+]$  are clamped by the pipette. The fact that large  $I_{sK}$  channel currents were observed under conditions which blocked basolateral  $K^+$  uptake suggests that space clamping was quite effective, since the pipette was the only source of  $K^+$ .

Use of a  $Cl^-$ -free environment for recordings in the whole-cell patch clamp experiments served three purposes. The first, mentioned in Materials and Methods, was the necessity to increase the cell membrane resistance to be able to clamp the cell voltage. The second was interference with all constitutive basolateral membrane transport processes involved in vectorial transport of  $K^+$ , allowing us to eliminate these as a source of the effects of cAMP. Third, it has been widely reported in many epithelia that a dominant effect of cAMP is the activation of  $Cl^-$  conductance. The demonstration of stimulation of  $I_{sK}$  channel current by cAMP in the absence of  $Cl^-$  argues against a  $Cl^-$  conductance as the basis of the observed effects.

Action of cAMP via changes in  $pH_i$  is also unlikely even though there is recent evidence that strongly suggests a potent activation of  $I_{sK}$  channels by intracellular acidification in vestibular dark cells [58]. The  $Na^+/H^+$ -exchanger in gallbladder epithelium is known to be inhibited by elevated cAMP, leading to acidification of the cytosol [36]. If this were the primary mode of action of cAMP in dark cells, however, it would be expected that the time constant of deactivation would have markedly increased, as found previously during acidification by

inhibition of the basolateral  $Na^+/H^+$ -exchanger with amiloride [61]. In contrast,  $\tau_{off}$  did not change during perfusion of dbcAMP, arguing against the involvement of cytosolic pH.

One common mechanism employed by secretory epithelia to regulate ionic current is to change the number of transport protein molecules in the cell membrane by inserting and removing protein via exocytosis and endocytosis [1]. Membrane traffic is often under control of the cAMP pathway in other epithelial cells such as a colonic epithelial cell line [7]. In vestibular dark cells, two types of vesicles (coated and uncoated) were observed in the vicinity of the apical membrane [23]. In dark cells of the frog, application of antidiuretic hormone stimulated cAMP production [16] and caused the appearance of numerous small vesicles in the apical cytoplasm [35], suggestive of a role in controlling membrane traffic. Subcellular localization of the  $I_{sK}$  channel protein has not yet been reported but it is conceivable that one mode of regulation of  $I_{sK}$  channel current in vestibular dark cells is the control of membrane traffic by cAMP.

Although the monophasic stimulatory effect of IBMX on  $I_{sK}$  in macropatch experiments was nearly identical to that of dbcAMP, it is not clear why the response of  $I_{sc}$  to IBMX in the micro-Ussing chamber was multiphasic, showing an apparent superimposed inhibition.  $I_{sK}$  has previously been shown to behave in a manner identical to  $I_{sc}$  under a variety of conditions including basolateral bumetanide, elevation of  $[K^+]$ , osmotic challenge and apical DIDS [26, 27, 39, 57]. The monophasic increase of  $I_{sK}$  observed in response to IBMX could be a result of not resolving the initial transient decrease and of a broadening of the stimulatory response. This may have occurred as a result of a combination of the low sampling rate of patch clamp data dictated by the required voltage protocol and of the slower perfusion rate in conjunction with the folded tissue geometry necessary to carry out the patch clamp experiments.

The cytoplasmic cAMP concentration is controlled by two processes, synthesis utilizing adenylate cyclases and catalysis via phosphodiesterases. Multiple subtypes of both enzymes have been found and their activity is susceptible to a variety of intracellular signalling pathways [4, 13]. The initial stimulation of  $I_{sc}$  by IBMX and Ro-20-1724 is likely due to elevation of cAMP and suggests a constitutive activity of cAMP production and degradation in vestibular dark cells. The putative receptors which control the cAMP pathway in vestibular dark cells remain to be determined although cAMP is increased in vestibular dark cells of frog semicircular canal by receptor agonists such as vasotocin and isoproterenol [16] and isoproterenol was recently found to stimulate  $I_{sc}$  in dark cells of gerbil [56].

IBMX has been widely recognized not only as a blocker of phosphodiesterase but also as a blocker of

adenosine  $P_1$  receptors [4]. We recently showed, however, that even though vestibular dark cells possess  $P_{2U}$  receptors in the apical membrane and coexisting  $P_{2Y}$  and  $P_{2U}$  receptors in the basolateral membrane, no evidence was found for  $P_1$  receptors coupled to  $I_{sc}$  [24]. It is therefore unlikely that IBMX affected these cells via  $P_1$  receptors.

In summary, the simplest interpretation of our data is that dbcAMP stimulates  $K^+$  secretion via a cellular rather than a paracellular pathway and that the stimulated current is carried by the apical  $I_{sK}$  channels. The results with IBMX and Ro-20-1724 suggest that there is constitutive cAMP metabolism. Similar responses of  $I_{sc}$  and the  $I_{sK}$  channels to dbcAMP and IBMX have been found recently in marginal cell epithelium from the stria vascularis in the cochlea [43], further strengthening the proposition that marginal cells and dark cells are functionally homologous. In addition to its importance in understanding the cellular regulation of inner ear function, these findings present evidence of upregulation of  $I_{sK}$  channel current in a native mammalian epithelium expressing an endogenous  $I_{sK}$  channel.

The authors thank Dr. Philine Wangemann for many helpful discussions and a critical reading of the manuscript. This work was supported by research grant number 5 R01 DC00212 from the National Institute on Deafness and Other Communication Disorders, National Institutes of Health.

## References

- Al Awqati, Q. 1989. Regulation of membrane transport by endocytotic removal and exocytotic insertion of transporters. *Methods Enzymol.* **172**:49–59
- Attali, B., Guillemare, E., Lesage, F., Honoré, E., Romey, G., Lazdunski, M., Barhanin, J. 1993. The protein IsK is a dual activator of  $K^+$  and  $Cl^-$  channels. *Nature* **365**:850–852
- Bakker, R., Groot, J.A. 1989. Further evidence for the regulation of the tight junction ion selectivity by cAMP in goldfish intestinal mucosa. *J. Membrane Biol.* **111**:25–35
- Beavo, J.A., Reifsnnyder, D.H. 1990. Primary sequence of cyclic nucleotide phosphodiesterase isozymes and the design of selective inhibitors. *Trends. Pharmacol. Sci.* **11**:150–155
- Ben-Efraim, I., Shai, Y., Attali, B. 1996. Cytoplasmic and extracellular IsK peptides activate endogenous  $K^+$  and  $Cl^-$  channels in *Xenopus* oocytes—Evidence for regulatory function. *J. Biol. Chem.* **271**:8768–8771
- Blumenthal, E.M., Kaczmarek, L.K. 1992. Modulation by cAMP of a slowly activating potassium channel expressed in *Xenopus* oocytes. *J. Neurosci.* **12**:290–296
- Bradbury, N.A., Jilling, T., Kirk, K.L., Bridges, R.J. 1992. Regulated endocytosis in a chloride secretory epithelial cell line. *Am. J. Physiol.* **262**:C752–C759
- Breton, S., Beck, J.S., Laprade, R. 1994. cAMP stimulates proximal convoluted tubule  $Na^+K^+$ -ATPase activity. *Am. J. Physiol.* **266**:F400–F410
- Busch, A.E., Herzer, T., Wagner, C.A., Schmidt, F., Raber, G., Waldegger, S., Lang, F. 1994. Positive regulation by chloride channel blockers of  $I_{sK}$  channels expressed in *Xenopus* oocytes. *Mol. Pharmacol.* **46**:750–753
- Busch, A.E., Lang, F. 1993. Effects of  $Ca^{2+}_i$  and temperature on minK channels expressed in *Xenopus* oocytes. *FEBS Lett.* **334**:221–224
- Busch, A.E., Varnum, M., Adelman, J.P., North, R.A. 1992. Hypotonic solution increases the slowly activating potassium current  $I_{sK}$  expressed in *xenopus* oocytes. *Biochem. Biophys. Res. Commun.* **184**:804–810
- Chang, X.B., Tabcharani, J.A., Hou, Y.X., Jensen, T.J., Kartner, N., Alon, N., Hanrahan, J.W., Riordan, J.R. 1993. Protein kinase A (PKA) still activates CFTR chloride channel after mutagenesis of all 10 PKA consensus phosphorylation sites. *J. Biol. Chem.* **268**:11304–11311
- Cooper, D.M., Mons, N., Karpen, J.W. 1995. Adenylyl cyclases and the interaction between calcium and cAMP signalling. *Nature* **374**:421–424
- Duffey, M.E., Hainau, B., Ho, S., Bentzel, C.J. 1981. Regulation of epithelial tight junction permeability by cyclic AMP. *Nature* **294**:451–453
- Fenwick, E.M., Marty, A., Neher, E. 1982. A patch-clamp study of bovine chromaffin cells and of their sensitivity to acetylcholine. *J. Physiol.* **331**:577–597
- Ferrary, E., Oudar, O., Bernard, C., Friedlander, G., Feldmann, G., Sterkers, O. 1991. Adenylate cyclase in the semicircular canal. Hormonal stimulation and ultrastructural localization. *Acta Otolaryngol.* **111**:281–285
- Freeman, L.C., Kass, R.S. 1993. Delayed rectifier potassium channels in ventricle and sinoatrial node of the guinea pig: molecular and regulatory properties. *Cardiovasc. Drugs Ther.* **7 Suppl** 3:627–635
- Haas, M., McBrayer, D.G., Yankaskas, J.R. 1993. Dual mechanisms for Na-K-Cl cotransport regulation in airway epithelial cells. *Am. J. Physiol.* **264**:C189–C200
- Hice, R.E., Folander, K., Salata, J.J., Smith, J.S., Sanguinetti, M.C., Swanson, R. 1994. Species variants of the  $I_{sK}$  protein: Differences in kinetics, voltage dependence, and  $La^{3+}$  block of the currents expressed in *Xenopus* oocytes. *Pfluegers Arch.* **426**:139–145
- Honoré, E., Attali, B., Romey, G., Heurteaux, C., Ricard, P., Lesage, F., Lazdunski, M., Barhanin, J. 1991. Cloning, expression, pharmacology and regulation of a delayed rectifier  $K^+$  channel in mouse heart. *Embo J.* **10**:2805–2811
- Katano, Y., Endoh, M. 1990. Differential effects of Ro 20-1724 and isobutylmethylxanthine on the basal force of contraction and beta-adrenoceptor-mediated response in the rat ventricular myocardium. *Biochem. Biophys. Res. Commun.* **167**:123–129
- Kunzelmann, K., Gerlach, L., Froebe, U., Greger, R. 1991. Bicarbonate permeability of epithelial chloride channels. *Pfluegers Arch.* **417**:616–621
- Lim, D.J., Freilich, I.W. 1981. Ultrastructure of the stria vascularis, vestibular dark cells and endolymphatic sac following acute diuretic ototoxicity. *Scand. Audiol. Suppl.* **14 Suppl**:139–155
- Liu, J., Kozakura, K., Marcus, D.C. 1995. Evidence for purinergic receptors in vestibular dark cell and stria marginal cell epithelia of gerbil. *Auditory Neurosci.* **1**:331–340
- Marcus, D.C., Liu, J., Sunose, H., Shen, Z. 1996. Protein kinase C mediates  $I_{sK}$  (min K) channel down-regulation by apical  $P_{2U}$  purinoceptor in  $K^+$ -secretory epithelial cells of the inner ear. *J. Gen. Physiol.* **108**:26a (Abstr.)
- Marcus, D.C., Liu, J., Wangemann, P. 1994. Transepithelial voltage and resistance of vestibular dark cell epithelium from the gerbil ampulla. *Hear. Res.* **73**:101–108
- Marcus, D.C., Shen, Z. 1994. Slowly activating, voltage-dependent

- $K^+$  conductance is apical pathway for  $K^+$  secretion in vestibular dark cell epithelium. *Am. J. Physiol.* **267**:C857–C864
28. Marcus, D.C., Shen, Z., Ryan, A.F. 1996. Species differences of  $I_{sk}$  channel mRNA in gerbil and rat. *J. Gen. Physiol.* **108**:26a (Abstr.)
  29. Marcus, D.C., Shipley, A.M. 1994. Potassium secretion by vestibular dark cell epithelium demonstrated by vibrating probe. *Biophys. J.* **66**:1939–1942
  30. Marcus, D.C., Sunose, H. 1996. Apical  $I_{sk}$  channel current is stimulated by cAMP and inhibited by protein kinase C in inner ear  $K^+$ -secretory epithelial cells of gerbil. *Biophys. J.* **70**:A30 (Abstr.)
  31. Marcus, D.C., Takeuchi, S., Wangemann, P. 1993. Two types of chloride channel in the basolateral membrane of vestibular dark cell epithelium. *Hear. Res.* **69**:124–132
  32. Marcus, N.Y., Marcus, D.C. 1985. Transepithelial cation movements in gerbil utricles. *Am. J. Otolaryngol.* **6**:268–274
  33. Morel, F., Doucet, A. 1986. Hormonal control of kidney functions at the cell level. *Physiol. Rev.* **66**:377–468
  34. Mori, N., Sakagami, M., Fukazawa, K., Matsunaga, T. 1993. An immunohistochemical and electrophysiological study on Isk protein in the stria vascularis of the guinea pig. *Eur. Arch. Otorhinolaryngol.* **250**:186–189
  35. Oudar, O., Ferrary, E., Feldmann, G. 1991. Antidiuretic-hormone-induced morphological changes in the ampullary epithelium of the frog semicircular canal. *Eur. Arch. Otorhinolaryngol.* **248**:386–389
  36. Reuss, L., Petersen, K.U. 1985. Cyclic AMP inhibits  $Na^+/H^+$  exchange at the apical membrane of *Necturus* gallbladder epithelium. *J. Gen. Physiol.* **85**:409–429
  37. Sakagami, M., Fukazawa, K., Matsunaga, T., Fujita, H., Mori, N., Takumi, T., Ohkubo, H., Nakanishi, S. 1991. Cellular localization of rat  $I_{sk}$  protein in the stria vascularis by immunohistochemical observation. *Hear. Res.* **56**:168–172
  38. Schacht, J. 1985. Hormonal regulation of adenylate cyclase in the stria vascularis of the mouse. *Hear. Res.* **20**:9–13
  39. Shen, Z., Liu, J., Marcus, D.C., Shiga, N., Wangemann, P. 1995. DIDS increases  $K^+$  secretion through an  $I_{sk}$  channel in apical membrane of vestibular dark cell epithelium of gerbil. *J. Membrane Biol.* **146**:283–291
  40. Shen, Z., Marcus, D.C., Sunose, H., Chiba, T., Wangemann, P. 1997.  $I_{sk}$  channel in stria marginal cells: Voltage-dependence, ion-selectivity, inhibition by 293B and sensitivity to clofilium. *Auditory Neurosci.* **3**:215–230
  41. Sunose, H., Ikeda, K., Saito, Y., Nishiyama, A., Takasaka, T. 1993. Nonselective cation and Cl channels in luminal membrane of the marginal cell. *Am. J. Physiol.* **265**:C72–C78
  42. Sunose, H., Ikeda, K., Suzuki, M., Takasaka, T. 1994. Voltage-activated K channel in luminal membrane of marginal cells of stria vascularis dissected from guinea pig. *Hear. Res.* **80**:86–92
  43. Sunose, H., Liu, J., Marcus, D.C. 1995. Stimulation of  $I_{sk}$  channel current by cAMP in  $K^+$ -secretory epithelia of inner ear. *Sendai Symposium '95* **5**:73–76
  44. Süßbrich, H., Bleich, M., Ecke, D., Rizzo, M., Waldegger, S., Lang, F., Szabo, I., Lang, H.J., Kunzelmann, K., Greger, R., Busch, A.E. 1996. Specific blockade of slowly activating  $I_{sk}$  channels by chromanols - Impact on the of  $I_{sk}$  channels in epithelia. *FEBS Lett.* **396**:271–275
  45. Swanson, R., Hice, R.E., Folander, K., Sanguinetti, M.C. 1993. The  $I_{sk}$  protein, a slowly activating voltage-dependent  $K^+$  channel. *Seminars in The Neurosciences* **5**:117–124
  46. Takeuchi, S., Irimajiri, A. 1996. A novel, volume-correlated  $Cl^-$  conductance in marginal cells dissociated from the stria vascularis of gerbils. *J. Membrane Biol.* **150**:47–62
  47. Takeuchi, S., Marcus, D.C., Wangemann, P. 1992. Maxi  $K^+$  channel in apical membrane of vestibular dark cells. *Am. J. Physiol.* **262**:C1430–C1436
  48. Takumi, T., Ohkubo, H., Nakanishi, S. 1988. Cloning of a membrane protein that induces a slow voltage-gated potassium current. *Science* **242**:1042–1045
  49. Tohse, N. 1990. Calcium-sensitive delayed rectifier potassium current in guinea pig ventricular cells. *Am. J. Physiol.* **258**:H1200–H1207
  50. Tzounopoulos, T., Maylie, J., Adelman, J.P. 1995. Induction of endogenous channels by high levels of heterologous membrane proteins in *Xenopus* oocytes. *Biophys. J.* **69**:904–908
  51. Varnum, M.D., Busch, A.E., Bond, C.T., Maylie, J., Adelman, J.P. 1993. The min K channel underlies the cardiac potassium current  $I_{ks}$  and mediates species-specific responses to protein kinase. *Proc. Natl. Acad. Sci. USA* **90**:11528–11532
  52. Vetter, D.E., Mann, J.R., Wangemann, P., Liu, J., McLaughlin, K.J., Lesage, F., Marcus, D.C., Lazdunski, M., Heineman, S.F., Barhanin, J. 1996. Inner ear defects induced by null mutation of the *isk* gene. *Neuron* **17**:1251–1264
  53. Wang, K.W., Goldstein, S.A. 1995. Subunit composition of minK potassium channels. *Neuron* **14**:1303–1309
  54. Wang, K.W., Tai, K.K., Goldstein, S.A.N. 1996. MinK residues line a potassium channel pore. *Neuron* **16**:571–577
  55. Wangemann, P. 1995. Comparison of ion transport mechanisms between vestibular dark cells and strial marginal cells. *Hear. Res.* **90**:149–157
  56. Wangemann, P., Liu, J. 1996. Beta-adenergetic receptors but not vasopressin-receptors stimulate the equivalent short circuit current in  $K^+$  secreting inner ear epithelial cells. *J. Gen. Physiol.* **108**:31a (Abstr.)
  57. Wangemann, P., Liu, J., Shen, Z., Shipley, A., Marcus, D.C. 1995. Hypo-osmotic challenge stimulates transepithelial  $K^+$  secretion and activates apical  $I_{sk}$  channel in vestibular dark cells. *J. Membrane Biol.* **147**:263–273
  58. Wangemann, P., Liu, J., Shiga, N. 1995. The pH-sensitivity of transepithelial  $K^+$  transport in vestibular dark cells. *J. Membrane Biol.* **147**:255–262
  59. Wangemann, P., Marcus, D.C. 1990.  $K^+$ -induced swelling of vestibular dark cells is dependent on  $Na^+$  and  $Cl^-$  and inhibited by piretanide. *Pfluegers Arch.* **416**:262–269
  60. Wangemann, P., Marcus, D.C. 1992. The membrane potential of vestibular dark cells is controlled by a large  $Cl^-$  conductance. *Hear. Res.* **62**:149–156
  61. Wangemann, P., Shen, Z. 1996. The  $I_{sk}$  channel in the apical membrane of vestibular dark cells is regulated by cytosolic pH. *Assoc. Res. Otolaryngol.* **19**:51 (Abstr.)
  62. Yamagishi, T., Yanagisawa, T., Satoh, K., Taira, N. 1994. Relaxant mechanisms of cyclic AMP-increasing agents in porcine coronary artery. *Eur. J. Pharmacol.* **251**:253–262
  63. Yang, Y., Sigworth, F.J. 1995. The conductance of minK 'channels' is very small. *Biophys. J.* **68**:A22 (Abstr.)
  64. Zhang, Z.J., Jurkiewicz, N.K., Folander, K., Lazarides, E., Salata, J.J., Swanson, R. 1994.  $K^+$  currents expressed from the guinea pig cardiac  $I_{sk}$  protein are enhanced by activators of protein kinase C. *Proc. Natl. Acad. Sci. USA* **91**:1766–1770